Inorg. Chem. **2004**, *43*, 2252−2260

Chlorides, Oxochlorides, and Oxoacids of 1,8-Diphosphanaphthalene: A System with Imposed Close P···P Interaction

Petr Kilian, Heather L. Milton, Alexandra M. Z. Slawin, and J. Derek Woollins*

Department of Chemistry, University of St. Andrews, St. Andrews, Fife KY16 9ST, U.K.

Received November 25, 2003

Several new 1,8-diphosphanaphthalene oxochloro compounds and oxoacids were prepared and fully characterized. The new compounds are discussed in the broader context with other known congeners to demonstrate the variability of the diphosphanaphthalene scaffolding's bonding patterns. Three principal modes of interaction of the phosphorus moieties were observed in the series: bonding, bridging, and repulsive, resulting respectively in none, moderate, and substantial crowding and distortions. The unexpected dimeric diphosphaacenaphthene anion has been obtained from disproportionative hydrolysis of Nap(PCl_2)$_2$ (Nap = naphthalene-1,8-diyl).

Introduction

The special bonding geometry in peri-substituted naphthalenes has received much attention in the past decade. In the "ideal" peri geometry (i.e. planar, all angles 120°), the *peri*-carbon atoms (carbons in positions 1 and 8) reside at a nonbonding distance of 2.47 Å; the exocyclic bonds emanating from them are parallel so that this would also be the ideal distance of the peri substituents. As the double of the van der Waals radii for essentially any pair of non-hydrogen atoms exceeds 2.5 Å, peri substitution always results in a crowded geometry if the peri atoms interact repulsively (as opposed to a bonding or bridging interaction). The crowded molecules adjust to the strain by spreading it over many coordinates, which is experimentally observed as twisting or bending of aromatics and exo bonds, on the one hand, and considerable sub van der Waals contacts on the other hand. Furthermore, the supporting effect of the rigid organic backbone in derivatives with direct P−P bond or P−X−P bridging is obvious and often facilitates stabilization of unusual bonding.

A few *peri*-diphosphanaphthalene chlorides, oxochlorides, and oxoacids are known; however, they are scattered in various papers by us as well as by other authors.[1−5] We report here the preparation and characterization of several new congeners (**3a**, **3b**, **5b**, **6**, **7**, and **8**; see Chart 1, Schemes 4 and 5). As these new derivatives fit well into the series, we shall discuss them in the broader context of those known as well as those missing members of the series aiming to emphasize and clarify the differences between predicted and observed reactivity, structure, and bonding.

Results and Discussion

The range of known as well as missing 1,8-diphosphanaphthalene chlorides, oxochlorides, and oxoacids, divided into groups according to the valencies of their phosphorus atoms, is shown in Chart 1. Only the "predictable" congeners with phosphorus atoms in the usual valencies (P^V and P^{III}) are shown.

1,8-Diphosphanaphthalene Chlorides NapP_2Cl_x. Attempts to prepare the bis(phosphorane) Nap(PCl_4)$_2$ **1a** (Nap = naphthalene-1,8-diyl) from the easily accessible phosphonium−phosphoride Nap(PCl_4)(PCl_2) **1b** by prolonged chlorination were unsuccessful;[1] **1b** thus represents the highest coordination, achievable by direct chlorination. Indeed, on the grounds of steric hindrance we consider **1a** as hypothetical only. The mutual contacts of phosphorus functionalities would require either extreme distortion of the phosphorus atoms' environment (toward pseudo-octahedral configuration) or excessive twisting of the organic backbone should the tbp configuration of phosphorus atoms be preserved.

Phosphonium−phosphoride **1b** displays a rare σ^4P−σ^6P bonding interaction with an unusually long P−P bond (2.34

* Corresponding author. E-mail: jdw3@st-andrews.ac.uk. Phone: (+44) 1334 463861. Fax: (+44) 1334 463384.

(1) Kilian, P.; Philp, D.; Slawin, A. M. Z.; Woollins, J. D. *Eur. J. Inorg. Chem.* **2003**, 249−254.
(2) Karacar, A.; Thonnessen, H.; Jones, P. G.; Bartsch, R.; Schmutzler, R. *Chem. Ber./Recl.* **1997**, *130*, 1485−1489.
(3) Kilian, P.; Slawin, A. M. Z.; Woollins, J. D. *Chem. Eur. J.* **2003**, *9*, 215−222.
(4) Kilian, P.; Slawin, A. M. Z.; Woollins, J. D. *Chem. Commun.* **2003**, 1174−1175.
(5) Kilian, P.; Touzin, J.; Marek, J.; Woollins, J. D.; Novosad, J. *Main Group Chem.* **1996**, 425−429.

10.1021/ic035364h CCC: $27.50
Published on Web 03/02/2004

Chart 1. Predicted Chloro-, Chloro-oxo-, and Oxoacids of Peri-diphosphanaphthalenes with Trivalent or Pentavalent Phosphorus Atoms[a]

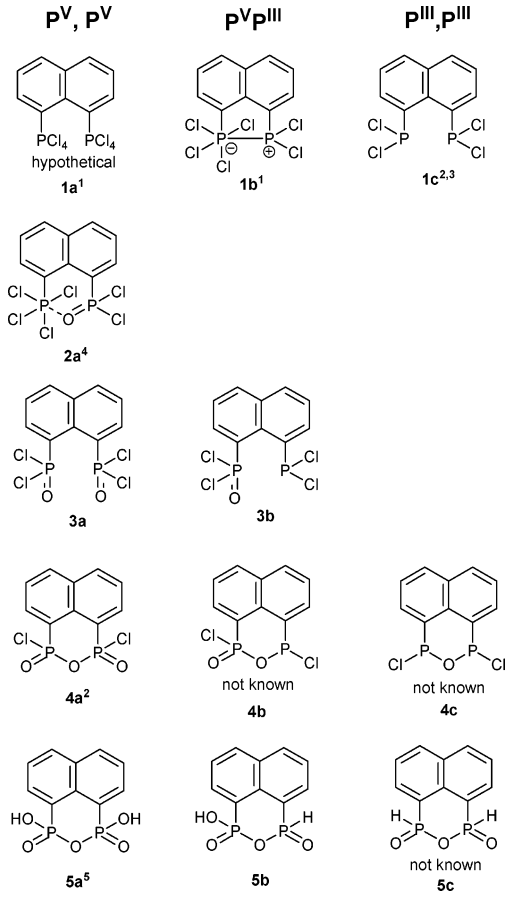

[a] The congeners are divided according to the valency of their phosphorus atoms, derivatives reported previously are referenced.

Å), clearly facilitated by the stiff backbone. Migration of chlorine atoms in the solutions of **1b** gives rise to interesting fluxionality on the NMR time scale. There is an exchange between the phosphonium−phosphoride $Nap(PCl_4)(PCl_2)$ and the bis(phosphorane) $Nap(PCl_3)(PCl_3)$ structures with preservation of the P−P bond throughout the process.[1]

Bis(dichlorophosphane) $Nap(PCl_2)_2$ **1c** shows a repulsive interaction of the phosphorus moieties; steric strain introduced by substitution in the peri region is eased by out-of-plane and in-plane distortions, concomitant with twisting of the naphthalene ring. As usual in such 1,8-diphosphanaphthalenes, the P atoms lie on opposite sides of the naphthalene plane (0.41 and 0.52 Å above and below it) and the P1···P9 nonbonding distance 2.80 Å is significantly shorter than the double van der Waals radii of the phosphorus atom (2×1.80 Å).[3]

1,8-Diphosphanaphthalene Oxochlorides $NapP_2Cl_xO_y$. Oxochlorides **2a**, **3a**,**b**, and **4a**−**c** (Chart 1) are formally products of step by step metathesis of two Cl atoms by an O atom, starting from their parent halides.

Only two of the six possible 1,8-diphosphanaphthalene oxochlorides have been previously reported, these being **2a** and **4a**.[2,4] The phosphorano−phosphine oxide $Nap(POCl_2)(PCl_4)$ **2a** displays interesting zwitterionic bonding enforced by the stiff backbone. Although the resulting O→P DA bond

Scheme 1

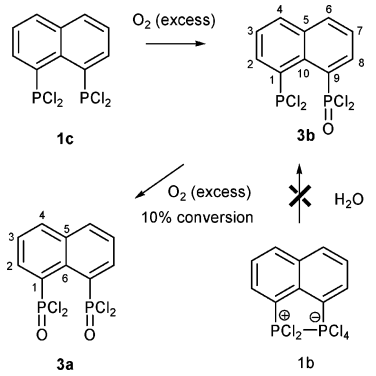

is relatively long (1.84 Å), it displayed an exceptionally high magnitude of $^2J(PP) = 64$ Hz. Phosphonyl halides may be obtained from the phosphonous halide by oxidation with oxygen gas (e.g. $PhPCl_2 + {}^1/_2O_2 \rightarrow PhPOCl_2$).[6] As mentioned in an earlier communication, this strategy was not successful here and **2a** was not accessible by oxidation of **1b** with O_2 or O_3. An alternative strategy was used [chlorination of $Nap(POCl_2)(PCl_2)$ **3b**], giving the desired product **2a** in a good yield.[4]

There were two options for the preparation of the next two congeners bis(phosphine oxide) $Nap(POCl_2)_2$ **3a** and mixed valence compound $Nap(POCl_2)(PCl_2)$ **3b**, these being the controlled hydrolysis of $NapP_2Cl_6$ **1b** and oxidation of bis(phosphine) **1c** with oxygen. The stoichiometrically controlled low temperature (−40 °C, solvent DME) hydrolysis of $NapP_2Cl_6$ **1b** delivered only inseparable mixtures of hydrolytic products; thus our attention turned to the oxidation of **1c** with oxygen gas (Scheme 1).

Interestingly, while the first oxidation step takes place easily, the oxidation of the second phosphorus atom did not reach completion even after 2 days at 80 °C (toluene solution). We observed only 10% conversion to the dioxidized $Nap(POCl_2)_2$ **3a** by ^{31}P NMR; on the other hand as well as the major product $Nap(PCl_2)(POCl_2)$ **3b** the mixture also contained small amounts of oxidation/hydrolysis product $NapP_2O_3Cl_2$ **4a**. A combination of sublimation and crystallization techniques were used for the separation of the resulting mixture, affording small amounts of pure **3a** and only slightly impure **3b**. The two new compounds **3a** and **3b** were fully characterized by X-ray crystallography, ^1H, ^{31}P, and ^{13}C NMR, IR, Raman, and MS, and the purity of **3a** was verified by microanalysis.

While **3a** showed the expected $^{31}P\{^1H\}$ spectrum (singlet δ 38.8), interesting features were observed in the $^{31}P\{^1H\}$ NMR spectrum of **3b**. On the basis of analogy with other mixed valence bay-substituted 1,8-diphosphanaphthalenes without any bonding interaction between the two phosphorus atoms, we expected the $^{31}P\{^1H\}$ NMR spectrum of **3b** to be an AX system with a small $^4J(PP)$. Measurement of the spectra of **3b** (in toluene, 109.4 MHz, 298 K) showed that the chemical shifts of both phosphorus atoms were as

(6) Corbridge, D. E. C. *Phosphorus, An Outline of its Chemistry, Biochemistry and Technology*, 3rd ed.; Elsevier: New York, 1985; p 232.

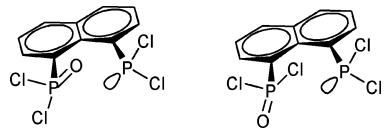

Figure 1. Plausible conformations observed as separate signals in $^{31}P\{^1H\}$ NMR spectra of **3b** due to restricted rotation about P−C bonds.

Scheme 2

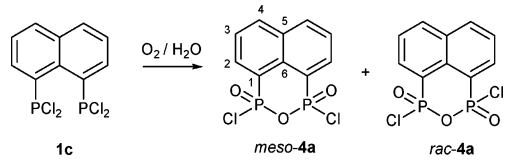

expected; however, the proposed AX pattern was found only in its low frequency half-spectrum (P^V, doublet at δ 41.7, J = 4.2 Hz). The high frequency signal (P^{III}) was composed of two poorly resolved, overlapping doublets at δ 146.2. Their pattern was virtually unchanged at low temperatures, though the peaks slightly sharpened, probably due to the natural line width narrowing with decreasing temperature. The measurement at 233 K (toluene, 109.4 MHz) showed that the P^{III} chemical shifts of the two isomeric forms are very similar (δ_{PIII} 145.52 and 145.50) and the P^V signal retains a pure doublet pattern (δ_{PV} 42.9). The integral ratio of the two forms was ca. 3:2; ^4J(PP) was for both isomeric forms identical (5.01 Hz). No signs of splitting were observed in ^1H or ^{13}C NMR spectra, though. We interpret the observed features as hindered rotation of PCl_2 and $POCl_2$ groups about the P−C bonds, resulting in the presence of at least two conformers whose interconversion is slow on the NMR time scale at the temperatures studied. Diagrams of the two plausible conformations occupying the energy minima are shown in Figure 1. The discrete conformers were observed by NMR in the series of similar, but much bulkier σ^3,σ^4-substituted 1,8-diphosphanaphthalenes, e.g. $Nap(PPh_2)$-$(PPh_2Me)^+$.[7] However, even with these bulky groups "molecular cogwheel" character was preserved, the hindrance being insufficient to give rise to atropoisomerism (allowing the separation of the two forms).

A few crystals of one of the two diastereomeric forms of condensed bis(chlorophosphonate) *meso*-**4a** were obtained essentially accidentally by Schmutzler et al. Only the X-ray structure of *meso*-**4a** was reported, as the amount of sample available did not allow for further characterization.[2] It seemed desirable to develop a rational synthetic route to **4a** and obtain its complete spectral data. Although we tested several methods for the preparation of **4a** and found that it is accessible from various precursors (e.g. from **1b**), we conclude for two reasons that the method of choice is controlled oxidation/hydrolysis of $Nap(PCl_2)_2$ **1c** (Scheme 2). The advantages of this method are the simplicity of workup and reproducibility with which satisfactory yields of *meso*-**4a** are obtained. The preparative reaction utilizes the unexpected relative stability of **4a** toward further hydrolysis, probably partially a result of the stabilizing effect

Scheme 3

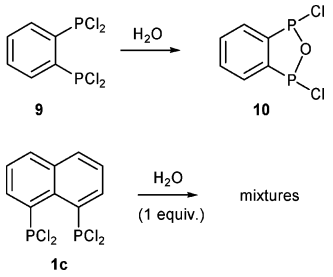

of P−O−P bridging. The uniform appearance of crystals obtained from toluene solutions suggests that **4a** crystallizes solely as the *meso* form from this solvent; the similarity of the crystals with the X-ray structure published earlier[2] was checked by measurement of their cell parameters. The $^{31}P\{^1H\}$ NMR spectrum of a freshly prepared $CDCl_3$ solution from crystalline material showed that it contained less than 2% of the *rac* isomer. Epimerization of *meso*-**4a** to the mixture of its *meso* (δ_P 13.8) and *rac* (δ_P 14.8) isomers was relatively slow: the equilibrium ratio (ca. 47:53 *meso*:*rac*, in $CDCl_3$) was reached after several weeks at ambient temperature. The rate of epimerization was substantially accelerated by impurities, though. The δ_P values observed for *rac*- and *meso*-**4a** are in good agreement with the value found for end-group PhP(O)(Cl)−O− (δ_P 12), obtained from hydrolytical condensation reaction of $PhP(O)Cl_2$.[8] *meso*-**4a** was fully characterized by ^1H, $^{13}C\{^1H\}$, and $^{31}P\{^1H\}$ NMR, MS, IR, and Raman spectroscopy, and the purity was assessed by microanalysis. ^1H and $^{31}P\{^1H\}$ NMR spectra of *rac*-**4a** subtracted from its mixture with the *meso*-**4a** are also reported.

Although in the related *o*-diphosphabenzene system the partial hydrolysis of bis(dichlorophosphane) **9** yielded cyclic anhydride **10** in a good yield (Scheme 3),[9] the analogous reaction with $Nap(PCl_2)_2$ **1c** gave a complicated mixture of products. Because the partial hydrolysis of $NapP_2Cl_6$ **1b** also resulted in inseparable mixtures of products (Scheme 1), our attention turned to fully hydrolyzed products **5a**−**5c**. The preparative route to compounds **4b** and **4c** thus remains unknown; nevertheless the ^{31}P NMR spctra we obtained indicated the presence of some new σ^3P motifs in the mixtures [δ_P range close to δ_P 188 found in **10**].[9]

1,8-Diphosphanaphthalene Oxoacids $NapP_2O_x(OH)_y$ and Their Salts. The bis(phosphonic) anhydride **5a** was obtained by the treatment of dithiadiphosphetane disulfide with ethylene glycol at 140 °C, and its full characterization together with X-ray structure analysis was published earlier.[5] The P−O−P bridging motif is stabilized by the stiff naphtho backbone; no signs of rupture of the six-membered C_3P_2O heterocycle were observed even after it was refluxed in water.

A total hydrolysis of **1b** afforded mixed valence phosphonic−phosphinic anhydride **5b** in a good yield (Scheme 4). The crude product was found to be contaminated by **5a**, probably generated by disproportionation side reaction. The

(7) Karacar, A.; Klaukien, V.; Freytag, M.; Thonnessen, H.; Omelanczuk, J.; Jones, P. G.; Bartsch, R.; Schmutzler, R. *Z. Anorg. Allg. Chem.* **2001**, *627*, 2589−2603.

(8) Dillon, K. B.; Nisbet, M. P.; Waddington, T. C. *J. Chem Soc., Dalton Trans.* **1981**, 212−218.

(9) Worz, H.-J.; Quien, E.; Latscha, H. P. *Z. Naturforsch.* **1984**, *39b*, 1706−1710.

Scheme 4

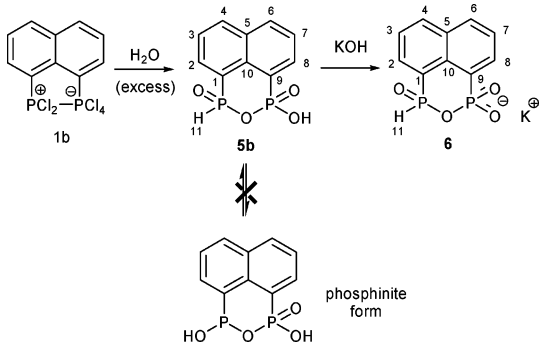

Scheme 5

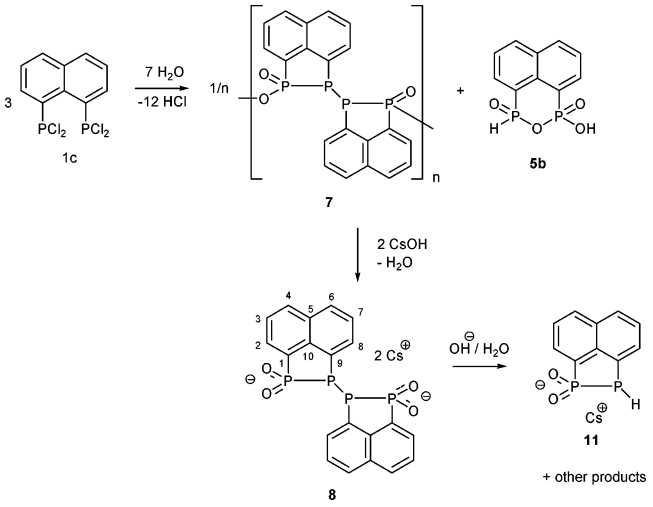

$^{31}P\{^{1}H\}$ spectrum of **5b** is an AX system with δ_{PV} 6.4 and δ_{PIII} 18.3, $^{2}J(PP) = 27.4$; measurement of a non-decoupled ^{31}P NMR experiment yielded $^{1}J(HP^{III}) = 626$ Hz. All these values are in very good agreement with phosphonic−phosphinic anhydride structure, as can be seen from the comparison with the corresponding parameters of anhydride **5a** (δ_P 6.6)[5] *o*-phenylene(bisphosphinic) acid *o*-C_6H_4[P(O)H(OH)]$_2$ (δ_P 14.3) [9] and *o*-phenylene phosphano−phosphinic acid *o*-$C_6H_4(PPh_2)$[P(O)H(OH)] (δ_P 22.6 and −15.3).[10] Further support of the proposed structure was provided by observation of rather quick proton−deuterium exchange of phosphorus-bonded hydrogen (in CD_3OD); the ^{31}P NMR spectrum of **5b** measured immediately after the preparation of the sample showed that the equilibrium ratio of deuterated and nondeuterated forms was already reached. Separate signals of both forms observed by ^{31}P NMR (109.4 MHz) show that the exchange is, however, slow on the NMR time scale. No signal in the usual range of σ^3 bonded phosphorus was observed, indicating that the possible phosphonite−phosphinite equilibrium (Scheme 4) is shifted completely to the phosphonite side in solutions of **5b**. Due to difficulties with further purification of a free acid **5b**, only the NMR characterization was performed, but the potassium salt $NapP_2O_4HK$ **6**, obtained by titration of the free acid with a solution of KOH, was fully characterized.

The decreased solubility of potassium salt **6** over free acid **5b** allowed its recrystallization from methanol/ethanol, affording **6** free of dioxidized byproduct **5a**. The NMR parameters of **6** are essentially identical to those of **5b**, the only change on deprotonation being a slight high-frequency shift of the P^{III} signal (δ_{PIII} 18.3 → 22.2). As expected the proton−deuterium exchange after dissolving **6** in D_2O was much slower than for the free acid **5b**, its rate being dependent on the acidity of the solution. Nevertheless, distinguishable amounts of the deuterated form were observed by ^{31}P NMR after several hours in D_2O solution. Other spectroscopic techniques afforded further support of proposed structure **6**; characteristic bands at 2394 (IR) and 2397 cm^{-1} (Raman) were assigned to ν_{P-H} vibrations; very good agreement with the proposed structure was also obtained in the ESI mass spectra in both positive and negative ionization modes, including exact mass measurement. The purity of **6** was verified by microanalysis. Attempts to precipitate **6** from water solution as salts by addition of $(Ph_4P)Cl$, $(n\text{-}Bu_4N)Cl$, or paraquat failed; salts of **6** with these cations were very soluble in water.

Hydrolysis of phosphonous chlorides $RPCl_2$ can proceed disproportionatively yielding primary phosphine RPH_2 and phosphonic acid $RP(O)(OH)_2$ if it is performed at ambient temperature; by lowering the reaction temperature the disproportionation is suppressed and the sole product is phosphinic acid RPH(O)(OH). Low temperature hydrolysis of **1c** unexpectedly occurs via the relatively complicated disproportionative mechanism, affording products **5b** and **7** (Scheme 5). Various signals of minor side products were detected by ^{31}P NMR in the reaction mixtures after hydrolysis of **1c** and after reaction of **7** with CsOH; however, none were unambiguously assignable to bis(phosphinic) anhydride **5c**.

Tetraphosphane Polymer $(Nap_2P_4O_3)_n$ and Cesium Salt $Cs_2(NapP_2O_2)_2$. Slow hydrolysis of $Nap(PCl_2)_2$ **1c** at ambient temperature resulted in complicated mixtures. Much cleaner reaction was observed by ^{31}P NMR when the reaction was performed at low temperature (−80 °C), although even so variable quantities of unidentified side products were sometimes observed. We ascribe this behavior to the sensitivity of the reaction to temperature; particularly the slow heating up from −80 °C to ambient temperature seemed to be critical. When performed appropriately, the reaction afforded two major phosphorus containing products. Very soluble **5b** was identified by ^{31}P and ^{1}H NMR spectroscopy (full characterization was performed on **5b** obtained by an independent method, vide infra), while the structure of a white precipitate (**7**) easily separable by filtration was deduced only after its conversion to soluble alkaline metal salt (vide supra; Scheme 5). Because of the insolubility of **7** in common solvents, no further purification was possible and only IR and MS spectra were recorded. The EI mass spectrum of **7** (sampled neat) consisted of nonassignable peaks only (probably from impurities), suggesting the polymeric nature of **7**. The IR spectrum contained very weak bands in the νOH region (again probably from impurities), while the νP═O and νP−O−P bands were very strong, in agreement with the proposed polymeric structure of **7**. More sophisticated support of the

(10) Kottsieper, K. W.; Kuhner, U.; Stelzer, O. *Tetrahedron: Asymmetry* **2001**, *12*, 1159−1169.

Scheme 6 Example of Diphospha-*o*-phenylene Dimer with Interleaved Geometry of *o*-$C_6H_4P_2$ Units

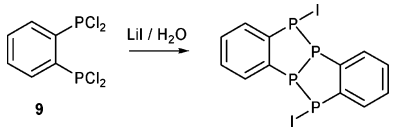

constitution of **7** was identification of the product of its alkaline hydrolysis (**8**).

Slow addition of cesium hydroxide solution to polymer **7** suspended in water resulted in the dissolution of the solid, yielding (water and methanol soluble) cesium salt **8** after evaporation (Scheme 5). The X-ray structure analysis of pale yellow crystals of *rac*-**8** showed that its dianionic part contains two naphthalene units connected together, forming a contiguous chain of four phosphorus atoms, the inner two having polyphosphine-like environments (formal oxidation state +I), while the terminal atoms are best described as oxidophosphoryl environments (oxidation state +IV). Compound *rac*-**8** represents the first crystallographically characterized example of a polyphosphane-like molecule with a naphthalene-1,8-diyl backbone. Unlike the *o*-phenylene-diphosphane based molecules, showing interleaved chaining of their monomeric units (Scheme 6),[11−13] *rac*-**8** displays head-to-head formation of homoatomic chains, obviously as a result of the rigid geometry and closeness of the phosphorus atoms in the diphosphanaphthalene units.

The $^{31}P\{^1H\}$ NMR spectrum of **8** in MeOH consists of two AA′XX′ systems, the presence of two chiral centers per molecule giving rise to two diastereomeric forms of **8** (93% and 7% abundance found in MeOH, the ratio did not change on standing of the solution). Iterative simulation of the spectra allowed for the determination of chemical shifts of the two forms (major diastereomer, δ_{PI} −77.9 and δ_{PIV} 52.8; minor, δ_{PI} −79.7 and δ_{PIV} 55.6); the calculation of a complete set of *J*(PP) was performed for the major diastereomer, giving magnitudes of the two ^1J(PP) of −245.5 (P^IP^I) and −136 Hz (P^IP^{IV}). The relatively low frequency shift δ_{PI} is not surprising as the polyphosphine-like phosphorus environments are known to display a very wide range of chemical shifts, the shielding of phosphorus nuclei being strongly dependent on organic substituent, bond angles, and even configuration. The chemical shift observed for the oxidophosphoryl environment in **8** is in good agreement with that observed for terminal phosphorus atom in a family of esters *t*-BuP[P(O)(OR^1)R^2] (R^1, R^2 = alkyl; δ_{PIV} 56.3−71.2).[14] The salt **8** was further characterized by ^{1}H and ^{13}C NMR, IR, Raman, and MS, and its purity was assessed by microanalysis. Compound **8** is very sensitive toward oxygen: even short exposure of the solution of **8** in methanol to air resulted in extensive oxidation.

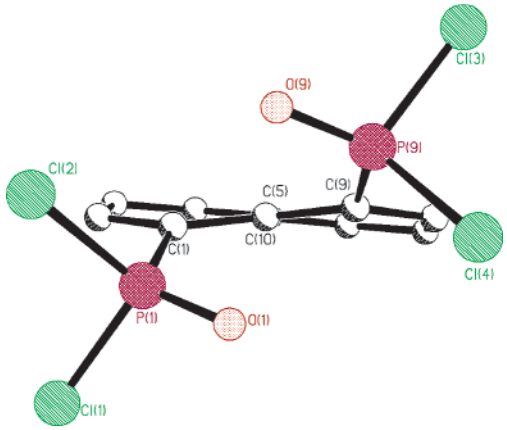

Figure 2. The structure of **3a** in the crystal. Naphthalene hydrogen atoms are omitted for clarity. Molecule is viewed along C(10)−C(5) bond to illustrate the extent of naphthalene ring twisting and out-of-plane distortions of phosphorus functionalities.

Neutral hydrolysis of diphosphanes R_2P-PR_2 is known to be slow at room temperature, but, under alkaline conditions, the P−P bond is broken with formation of secondary phosphane R_2PH and unstable phosphinous acid $R_2P(OH)$, undergoing tautomeric change to tetrahedral phosphane oxide $R_2PH(O)$. As there are some similarities in the bonding of the two naphthalene subunits in **8** and in diphosphanes, we expected a similar decomposition pathway under alkaline conditions. In fact, when an excess of hydroxide was used in reaction with polymer **7**, decomposition of **8** was observed, leading to several products. Unfortunately, from these only phosphane **11** could be identified tentatively from its $^{31}P\{^1H\}$ and ^{31}P NMR spectra (Scheme 5).[15]

Crystallographic Discussion. The structures of compounds **3a** and **3b** in the crystal are shown in Figures 2 and 3 and Tables 1 and 3. Both crystallize with one molecule in the asymmetric unit. The molecule of dioxide **3a** possesses a noncrystallographic 2-fold axis along the C(5)−C(10) bond; no symmetry element is present in monoxide **3b**. The different substitution pattern of phosphorus atoms in **3b** results in slightly different P−C bond lengths [P^{III}−C(1) 1.838(3) Å and P^V−C(9) 1.788(3) Å]. Both structures display distinct twisting of the backbone with phosphorus atoms being displaced to opposite faces of the best naphthalene plane. The positive values of splay angle clearly indicate repulsive interactions of phosphorus moieties concomitant with clearly distinguishable in-plane distortions. Steric strain is relatively high in both molecules, though not surprisingly the distortions are more pronounced in the dioxide **3a** than in the monoxide **3b**. This is indicated by difference in the length of the P···P contacts [3.475(4) Å in **3a** and 3.168(1) Å in **3b**] as well as by other distortion descriptive parameters such as the displacement of the phosphorus atoms from naphthalene mean plane and the central naphthalene torsion angles (see Table 1). Both molecules occupy the conformation with sterically less demanding oxygen atom(s) located

(11) Stritt, H.-P.; Worz, H.-J.; Latscha, H. P. *Z. Naturforsch.* **1985**, *40b*, 1711−1714.
(12) Worz, H.-J.; Pritzkow, H.; Latscha, H. P. *Z. Naturforsch.* **1984**, *39b*, 139−141.
(13) Etkin, N.; Fermin, M. C.; Stephan, D. W. *J. Am. Chem. Soc.* **1997**, *119*, 11420−11424.
(14) Kabachnik, M. M.; Novikova, Z. S.; Lutsenko, I. F. *Zh. Obsch. Khim.* **1982**, *52*, 763−768; *J. Gen. Chem. USSR (Engl. Transl.)* **1982**, *52*, 662−666.
(15) NMRs of **11** in MeOH at 109.4 MHz: $^{31}P\{^1H\}$ 2 × d, δP −123.8 and 54.0, ^1J(PP) = 109.0; ^{31}P(nondecoupled) low-frequency signal split by directly bonded proton, ^1J(PH) = 192.7 Hz. Both the chemical shifts as well as relatively low magnitudes of ^1J(PH) and ^1J(PP) are in good agreement with proposed structure of **11**.

Table 1. Selected Bonding, Nonbonding, and Displacement Distances [Å] and Bond Torsion and Dihedral Angles [deg] for **3a** and **3b**[a]

compd	**3a**	**3b**[b]
substitution pattern	O, O	O, −
Peri-Region Distances and Short Contacts		
P(1)−C(1)	1.794(6)	1.838(3)
P(9)−C(9)	1.795(6)	1.788(3)
P(1)−O(1)	1.458(5)	
P(9)−O(9)	1.459(5)	1.444(3)
P(1)−Cl(1)	2.021(2)	2.045(1)
P(1)−Cl(2)	1.998(2)	2.079(1)
P(9)−Cl(3)	2.022(2)	2.023(1)
P(9)−Cl(4)	2.001(2)	2.000(1)
P(1)···P(9); % of Σr_{VdW}[c]	3.475(4); 96	3.168(1); 88
P(1)···O(9); % of Σr_{VdW}[c]	2.946(6); 89	2.668(3); 80
P(9)···O(1); % of Σr_{VdW}[c]	2.963(6); 89	
Out-of-Plane Displacement and Dihedral Angles		
P(1)	0.94	0.75
P(9)	0.95	0.78
P(1)−C(1)···C(9)−P(9)	49.4	39.2
Peri-Region Bond Angles		
splay angle[d]	13.0	7.7
P(1)−C(1)−C(10)	123.3(5)	119.5(2)
P(9)−C(9)−C(10)	121.6(4)	121.3(2)
C(1)−C(10)−C(9)	128.1(5)	126.9(3)
Central Naphthalene Ring Torsion Angles		
C(4)−C(5)−C(10)−C(1)	11.1	8.5
C(4)−C(5)−C(10)−C(9)	169.1	171.8

[a] For numbering of atoms, see Figures 2 and 3. [b] The oxygen atom in the structure of **3b** shows partial disorder. [c] The following values of van der Waals radii were used in calculations: $r_{VdW}(P) = 1.80$, $r_{VdW}(O) = 1.52$, $r_{VdW}(Cl) = 1.75$ Å. [d] Splay angle = P(1)−C(1)−C(10) + P(9)−C(9)−C(10) + C(1)−C(10)−C(1′) − 360.

in peri space, O···P and P···P contacts bearing a substantial portion of the strain [e.g. P(1)···O(9) contacts in **3b** are 80% of the sum of van der Waals radii of the atoms]. The attractive 3c-4e O···P−Cl interactions may also contribute to shortening of the P···O distances to sub van der Waals range, the respective O···P−Cl angles being 176.1° [O(1)···P(9)−Cl(3)] and 178.2° [O(9)···P(1)−Cl(1)] in **3a** and 177.3° [O(9)···P(1)−Cl(2)] in **3b**.[16] In **3b** the lone pair is located inside the peri space, although not pointing directly toward the other P atom. The overall steric strain in **3a** and **3b** is very similar to that found in Nap[P(O)(OMe)$_2$]$_2$ [P···P contacts 3.471(2) Å] and Nap[P(O)(OMe)$_2$][P(OMe)$_2$] [P···P contacts 3.238(4) Å];[17] the P···P distance in Nap(PCl$_2$)$_2$ **1c** [2.798(2) and 2.811(1) Å for the two molecules in the asymmetric unit][3] fits well into the series with **3a** and **3b** where a distinct increase of the distance with increased coordination of phosphorus atoms is observed.

The structure of *rac*-**8** in the crystal is shown in Figure 4 and Tables 2 and 3. The asymmetric unit contains the dianion, two cesium cations, and two molecules of methanol. The dianion possesses approximate C_2 symmetry, the noncrystallographic 2-fold axis being perpendicular to the P^{I}−P^{I} bond connecting the two diphosphaacenaphthene moieties. The two diphosphaacenaphthene mean planes are nearly parallel (the separation distance between them is approximately 2.2 Å), although mutual ca. 90° rotation of the two rings results in no overlap of the two aromatic systems. The relaxation of the crowded repulsive geometry on formation of the peri-region P−P bond results in essentially planar geometry of the NapP$_2$ subunits, the maximum distance of P atom from the naphthalene mean plane being 0.11 Å and the splay angles being negative (−7.3° and −7.5° for the two subunits). In agreement with an expected mild stretching effect of the naphthalene backbone, slightly elongated P−P bonds in C$_3$P$_2$ heterocycles [2.238(3) and 2.242(3) Å] compared to the interconnecting P−P bond [2.218(4) Å] were observed, though all three P−P bonds still lie in a narrow range (2.20 ± 0.05 Å) observed in wide variety of P−P bond containing compounds. Nearly identical P−P bond lengths were found in the other diphosphaacenaphthene systems Nap(PPh)$_2$[18] (σ^3P−σ^3P motif) and Nap(PR$^1_2$)$^+$-(PR^2) (R^1, R^2 = alkyl, Cl; σ^4P−σ^3P motif),[19] only the σ^6P−σ^4P system in **1b** showed a significantly longer P−P bond [2.338(2) Å], probably due to the increased crowding on hypercoordination of its phosphorus atom. The inner C−P−P angles in the C$_3$P$_2$ heterocycles of *rac*-**8** [90.9(3)−95.9(3)°] are reduced compared to the usual value of ca. 100° found in nonplanar five-membered heterocycles, indicating a slight increase of small-angle strain at phosphorus atoms on decreasing the nonbonding strain and angular strain in the organic backbone. The different substitution pattern of the two phosphorus atoms in each naphthalene entity results in subtle differences in the P−C bond lengths [P^{I}−C(9) 1.829(9) Å vs P^{IV}−C(1) 1.813(8) Å]. The negative charge is delocalized across each two oxygen atoms of the dianion as reflected by almost equal P−O bond lengths; both cesium atoms interact with all the oxygen atoms with Cs···O distances in the range 2.96−3.59 Å, the methanol solvate molecules coordinate to the Cs$^+$ centers. The molecules of *rac*-**8** pack with the naphthalene rings parallel to each other, though with a minimum of overlap between the adjacent rings. Layers of organic anions are interleaved with layers of cesium cations and molecules of solvated methanol.

Conclusions

A wide variety of binding/repulsive modes have been observed in 1,8-diphosphanaphthalene chlorides, oxochlorides, and oxoacids. Unusual enforced bonding interactions between the two phosphorus centers were found in the hypercoordinated chlorine-rich derivatives Nap(PCl$_4$)(PCl$_2$) **1b** and Nap(POCl$_2$)(PCl$_4$) **2a**. The less oxygen rich oxochlorides adopt strained repulsive geometry, while the presence of more hydroxyl groups leads to release of the strain by formal elimination of HCl (or H$_2$O) and formation of P−O−P bridging observed in NapP$_2$O$_3$Cl$_2$ **4a**. The last feature applies also to oxoacids, as documented by the P−O−P bridged structures (and stabilities) of bis(phosphonic) acid anhydride **5a** and phosphonic−phosphinic anhydride **5b**. The proximity of phosphorus atoms in the bifunctional molecular scaffolding results in interesting

(16) Nakanishi, W.; Hayashi, S. *Phosphorus, Sulfur Silicon Relat. Elem.* **2002**, *177*, 1833−1837.
(17) Kilian, P.; Slawin, A. M. Z.; Woollins, J. D. *Dalton Trans.* **2003**, 3876−3885.
(18) Mizuta, T.; Nakazono, T.; Miyoshi, K. *Angew. Chem., Int. Ed.* **2002**, *41*, 3897−3898.
(19) Karacar, A.; Freytag, M.; Thonnessen, H.; Jones, P. G.; Bartsch, R.; Schmutzler, R. *J. Organomet. Chem.* **2002**, *643*−*644*, 68−80.

Table 2. Selected Bonding, Nonbonding, and Displacement Distances [Å] and Bond, Torsion, and Dihedral Angles [deg] for *rac*-**8**[a]

Peri-Region Bond Lengths							
P(1)−C(1)	1.813(8)	P(9)−C(9)	1.829(9)	P(11)−C(11)	1.850(8)	P(19)−C(19)	1.797(9)
P(1)−P(9)	2.238(3)	P(9)−P(11)	2.218(4)	P(11)−P(19)	2.242(3)		
P(1)−O(1)	1.504(7)	P(1)−O(2)	1.503(6)	P(19)−O(3)	1.511(6)	P(19)−O(4)	1.504(7)

Out-of-Plane Displacement and Dihedral Angles			
P(1)	P(9)	P(11)	P(19)
P(1)−C(1)···C(9)−P(9)	2.8(4)	P(11)−C(11)···C(19)−P(19)	5.4(4)

Peri-Region Bond Angles					
P(1)−P(9)−P(11)	96.79(13)	P(9)−P(11)−P(19)	93.32(12)		
O(1)−P(1)−O(2)	115.9(3)	O(3)−P(19)−O(4)	116.1(3)		
P(1)−C(1)−C(10)	114.9(6)	P(9)−C(9)−C(10)	117.6(6)	C(1)−C(10)−C(9)	120.0(7)
P(19)−C(19)−C(20)	114.9(6)	P(11)−C(11)−C(20)	117.8(6)	C(11)−C(20)−C(19)	120.0(7)
P(1)−P(9)−C(9)	91.8(3)	P(9)−P(1)−C(1)	95.5(3)		
P(11)−P(19)−C(19)	95.9(3)	P(19)−P(11)−C(11)	90.9(3)		
P(9)−P(11)−C(11)	100.1(3)	P(11)−P(9)−C(9)	101.4(3)		

Central Naphthalene Torsion Angles			
C(1)−C(10)−C(5)−C(6)	177.2	C(1)−C(10)−C(5)−C(4)	1.34
C(11)−C(20)−C(15)−C(16)	179.1	C(11)−C(20)−C(15)−C(14)	2.63

[a] For numbering of atoms, see Figure 4.

Table 3. Crystallographic Data for **3a**, **3b**, and *rac*-**8**[a]

	3a	**3b**	*rac*-**8**
chemical formula	$C_{10}H_6Cl_4O_2P_2$	$C_{10}H_6Cl_4OP_2$	$C_{22}H_{20}Cs_2O_6P_4$
fw	361.89	345.89	770.08
cryst color, shape	colorless prism	colorless prism	yellow prism
cryst syst	monoclinic	monoclinic	triclinic
space group	$P2_1$	$P2_1/c$	$P\bar{1}$
a/Å	8.4511(4)	9.465(1)	7.157(5)
b/Å	10.6848(4)	16.035(2)	12.363(9)
c/Å	8.7458(5)	8.859(1)	14.69(1)
α/deg	90.00	90.00	109.05(1)
β/deg	118.143(2)	95.151(2)	90.52(1)
γ/deg	90.00	90.00	90.62(1)
V/Å^3, *Z*	696.36(6), 2	1339.2(3), 4	1228(1), 2
T/K	293(2)	125(2)	125(2)
D_{calcd}/g cm^{-3}	1.726	1.716	2.082
μ/mm^{-1}	1.067	1.100	3.266
R (F^2, all data)[b]	0.0519	0.0640	0.0652
wR (F^2, all data)[b]	0.1146	0.1045	0.1163

[a] All data were collected on a Bruker SMART CCD diffractometer equipped with Oxford Instruments low-temperature attachment, using Mo Kα radiation ($\lambda = 0.71073$ Å). [b] $R = \sum||F_o| - |F_c||/\sum|F_o|$; $wR = [\sum[w(F_o^2 - F_c^2)^2]/[\sum(F_o^2)^2]]^{1/2}$.

chemistry once more in the case of lower valent phosphorus oxoacids, as observed for the unexpected disproportionative hydrolysis mechanism of $Nap(PCl_2)_2$ **1c**, yielding the oligophosphine product $[(NapP_2O)_2O]_n$ **7**, fully characterized as cesium salt $Cs_2[(NapP_2O_2)_2]$ **8**.

Synthetic utility of the halogenophosphines $Nap(PCl_4)(PCl_2)$ **1b** and $Nap(PCl_2)_2$ **1c** is obvious; many potentially interesting derivatives (e.g. chiral phosphines) are commonly prepared using halogenophosphines as precursors. The dichloride $NapP_2O_3Cl_2$ **4a** seems to be a promising bifunctional synthon, e.g. for the preparation of new bicylic heterocycles; we also expect synthetic use of acid $NapP_2O_4H_2$ **5b** or potassium salt $K[NapP_2O_4H]$ **6**, respectively, due to the presence of a reactive P−H bond.

Experimental Section

All experiments were carried out in standard Schlenk glassware with exclusion of air and moisture. Solvents were dried, purified,

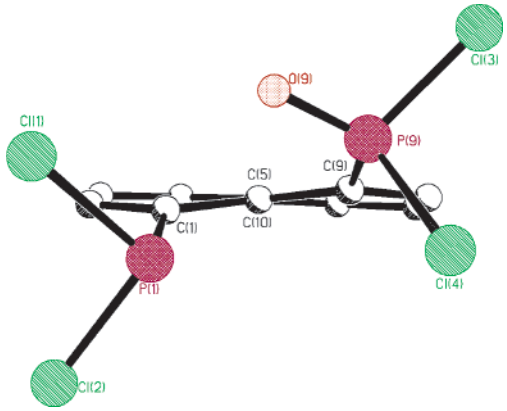

Figure 3. The structure of **3b** in the crystal. The oxygen atom shows partial disorder with 10% occupancy of position O(1) and 90% of position O(9). Naphthalene hydrogen atoms are omitted for clarity. Molecule is viewed along C(10)−C(5) bond to illustrate the extent of naphthalene ring twisting and out-of-plane distortions of phosphorus functionalities.

and stored according to common procedures;[20] water used in experiments was deoxygenated by prolonged bubbling of nitrogen through it. Phosphonium−phosphoride $Nap(PCl_4)(PCl_2)$ **1b** was prepared by chlorination of dithiadiphosphetane disulfide $NapP_2S_4$,[1] and bis(dichlorophosphane) $Nap(PCl_2)_2$ **1c** was obtained by the action of $MeOPCl_2$ on **1b**.[3] All other reagents were obtained commercially. In vacuo refers to pressure of ≈26 Pa. NMR: Bruker Avance 300 and JEOL GSX Delta 270; 85% H_3PO_4 was used as external standard in ^{31}P, TMS as internal in ^1H and ^{13}C NMR. All measurements were performed at 25 °C. Assignments of ^{13}C and ^1H NMR spectra were made with the help of $^1H\{^{31}P\}$, H−H COSY, H−C HMBC, H−C HSQC, and H−P HMQC experiments. Raman (sealed capillaries) and IR (KBr tablets or Nujol mull): Perkin-Elmer System 2000. MS: VG Autospec, electron energy 70 eV and Micromass LCT (ES). Microanalyses were performed by departmental service on a Carlo Erba CHNS analyzer.

Reaction of $Nap(PCl_2)_2$ (1c) with Oxygen Gas. A solution of $Nap(PCl_2)_2$ **1c** (2.31 g, 7.00 mmol) in toluene (10 cm^3) was placed into a 250 mL flask equipped with a rubber septum, cooled to −80 °C, and shortly evacuated. Dry oxygen gas (excess) was added using a balloon via septum, and the closed flask was heated to 80 °C for

(20) Perrin, D. D.; Armarego, W. L. F. *Purification of Laboratory Chemicals*, 3rd ed.; Pergamon Press: Oxford, 1988.

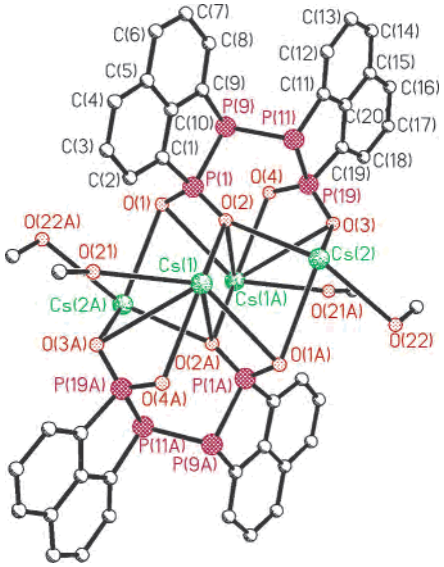

Figure 4. The structure of *rac*-**8** in the crystal. Two asymmetric units are shown to illustrate the bonding of cesium cations with oxygen atoms of anion and solvated methanol (two molecules per asymmetric unit).

2 days. The volatiles were removed in vacuo at room temperature, and the resulting solid was transferred into a sublimation apparatus and sublimed (140 °C, in vacuo), which led to the preseparation to $Nap(POCl_2)(PCl_2)$ **3b** (sublimate) and $Nap(POCl_2)_2$ **3a** (sublimation residue). Both fractions required further purification though.

$Nap(POCl_2)_2$ (3a). The less volatile fraction from sublimation above (sublimation residue) was recrystallized twice from hot toluene/hexane, yielding pure colorless crystalline **3a** (0.131 g, 5%). $C_{10}H_6Cl_4O_2P_2$: calcd C 33.2, H 1.7; found C 33.6, H 1.5. Mp: 252−255 °C with decomposition. IR (Nujol mull, cm^{-1}): ν = 1489m, 1256vs ($\nu_{P=O}$), 898s, 829s, 763vs, 582vs and 545s (ν_{PCl}), 506vs, 413vs. Raman (sealed capillary, cm^{-1}): ν = 3068m (ν_{Ar-H}), 1552s, 1341vs, 1263m ($\nu_{P=O}$), 554s, 418s. NMR ($CDCl_3$, for numbering of atoms see Scheme 1): ^{1}H (300 MHz) δ 7.71 (m, 2H, H3), 8.12 [m, 2H, ^3J(HH) = 8.3, ^4J(HH) = 1.1 Hz, H4], 8.39 [m, 2H, ^3J(HP) = 25.9, ^3J(HH) = 7.3, ^4J(HH) = 1.0 Hz, H2]; ^{13}C{^{1}H} (75.5 MHz) δ 126.4 [m (second order), C3], 129.2 [t, ^2J(CP) = 11.9 Hz, C6], 131.5 [dd, ^1J(CP) = 163.9, ^3J(CP) = 2.8 Hz, C1], 133.5 [t, ^3J(CP) = 14.6 Hz, C5], 136.1 [m (second order), C4], 138.1 [m (second order), C2]; ^{31}P{^{1}H} (121.5 MHz) δ 38.8(s), analysis of ^{13}C satellite subspectrum yielded ^4J(PP) ≈ 8.3 and confirmed ^1J(PC) = 163.9 Hz. MS (EI+): *m*/*z* 325 (M − Cl), 290 (M − 2Cl), 243 ($C_{10}H_6POCl_2$, base peak), 189 ($C_{10}H_7P_2$), 126 ($C_{10}H_6$).

$Nap(POCl_2)(PCl_2)$ (3b). The sublimate from the above reaction contained except the desired **3b** also small amounts of cosublimed **3a** and **4a**; however, it was of sufficient purity for further syntheses (yield 1.54 g, 64%). Further purification turned out to be rather difficult; the most pure product was obtained with repeated fractional crystallizations from hot toluene, affording **3b** contaminated only by ca. 10% of **3a** (**4a** was the least soluble compound in the system). The contaminated colorless crystalline solid **3b** was used for the following spectroscopic characterization. IR (Nujol mull, cm^{-1}): ν = 1248vs ($\nu_{P=O}$), 881s, 825s, 762vs, 577 and 547vs (ν_{PCl}), 499s, 475s, 445s. Raman (sealed capillary, cm^{-1}): ν = 3072m, 3053m (ν_{Ar-H}), 1553s, 1336vs, 1249m ($\nu_{P=O}$), 883m, 550s, 434s. NMR ($CDCl_3$, the signals of **3a** were abstracted, for numbering of atoms see Scheme 1): ^{1}H (300.1 MHz) δ 7.63 [m, 1H, ^4J(HP) = 3.8 Hz, H7], 7.73 [m, 1H, H3], 8.01 [m, 1H, ^3J(HH) = 8.3, ^4J(HH) = 1.2 Hz, H4], 8.12 [m, 1H, ^3J(HH) = 8.3, ^4J(HH) = 1.2 Hz, H6], 8.34 [ddd, 1H, ^3J(HP) = 24.9, ^3J(HH) = 7.4, ^4J(HH) = 1.3 Hz, H8], 8.76 [ddd, 1H, ^3J(HP) = 4.1, ^3J(HH) = 7.3, ^4J(HH) = 1.3 Hz, H2]; ^{13}C{^{1}H} (75.5 MHz) δ 125.2 [d, ^3J(CP) = 20.4 Hz, C7], 128.0 (s, C3), 129.4 [dd, ^1J(CP) = 150.9, ^3J(CP) = 1.7 Hz, C9], 131.5 [dd, ^3J(CP) ≈ 40.4 and 13.3 Hz, C5], 133.3 [dd, ^2J(CP) ≈ 14.9 and 6.1 Hz, C10], 134.2 [d, ^4J(CP) = 2.8 Hz, C4], 137.0 [d, ^2J(CP) = 13.8 Hz, C8], 137.4 [dd, ^4J(CP) = 4.4 and 1.7 Hz, C6], 138.6 [dd, ^2J(CP) = 3.9, ^4J(CP) = 1.7 Hz, C2], 140.6 [dd, ^1J(CP) = 71.3, ^3J(CP) ≈ 2 Hz, C1]; ^{31}P{^{1}H} (121.5 MHz, $CDCl_3$, 25 °C) δ 44.4 (d, P^V), 147.0 [m (poorly resolved), P^{III}], ^4J(PP) ≈ 3.0 Hz (read from low frequency doublet), for detailed analysis see text. MS (EI+): *m*/*z* 344 (M^+, correct isotopic pattern), 325 (M − Cl + O), 309 (M − Cl, base peak, correct isotopic pattern), 274 (M − 2Cl).

$NapP_2O_3Cl_2$ (4a). A 100 cm^3 flask equipped with a rubber septum, a containing solution of **1c** (0.60 g, 1.82 mmol) in toluene (10 cm^3), was shortly evacuated, and dry oxygen gas (50 cm^3, 2.23 mmol) was added by syringe. The solution was heated to 100 °C for 10 min; ^{31}P{^{1}H} NMR examination of the resulting pale yellow solution showed it to be a mixture of unreacted **1c**, monoxidized $Nap(POCl_2)(PCl_2)$ **3b** (major product), and dioxidized $Nap(POCl_2)_2$ **3a**. Slow hydrolysis was then performed by exposing the reaction mixture to air moisture via needle repeatedly placed through the rubber septum for several minutes (during a period of a few days). The least soluble compound in the system, *meso*-**4a**, precipitated gradually; it was filtered off, washed with toluene (2 × 2 cm^3) and recrystallized from hot toluene. Yield: 0.21 g (38%) of colorless crystalline *meso*-**4a**. $C_{10}H_6Cl_2O_3P_2$: calcd C 39.1, H 2.0; found C 39.3, H 1.9. Mp: 206−208 °C (*meso*-**4a**). IR (*meso*-**4**, Nujol mull, cm^{-1}): ν = 1497m, 1294, 1277vs ($\nu_{P=O}$), 966vs, 913vs, 609vs, 562, 546s (ν_{PCl}). Raman (*meso*-**4**, sealed capillary, cm^{-1}): ν = 3074m (ν_{Ar-H}), 1568s, 1359vs, 1297m, 1279m ($\nu_{P=O}$), 483s. NMR ($CDCl_3$, *meso* isomer, for numbering of atoms see Scheme 2): ^{1}H (300 MHz) δ 7.80 (m, 2H, H3), 8.27 [m, 2H, ^3J(HH) = 8.5, ^4J(HH) = 1.2 Hz, H4], 8.42 [m, 2H, ^3J(HH) = 7.2, ^4J(HH) = 1.2 Hz, H2]; ^{13}C{^{1}H} (67.9 MHz) δ 123.4 [m (second order), C1], 127.1 [t (virtual), C3], 127.4 [t, ^2J(CP) = 14.5 Hz, C6], 132.7 [t, ^3J(CP) = 15.0 Hz, C5], 135.1 [t (virtual), C2], 136.5 (s, C4); ^{31}P{^{1}H} (109.4 MHz) δ 13.8(s), combined analysis of ^{13}C satellites in ^{31}P{^{1}H} NMR spectrum and second-order signal of C1 yielded ^2J(PP) = 54, ^1J(P1C1) = 169 and ^3J(P9C1) = 4 Hz. NMR ($CDCl_3$, *rac* isomer, subtracted from mixture with *meso* isomer, the same numbering scheme as for *meso* isomer was used): ^{1}H (300 MHz) δ 7.82 (m, 2H, H3), 8.29 [m, 2H, ^3J(HH) = 8.5, ^4J(HH) = 1.1 Hz, H4], 8.43 [m, 2H, ^3J(HH) = 7.2, ^4J(HH) = 1.3 Hz, H2]; subtle changes of δ and *J* compared to the *Z* isomer were observed also in the ^{13}C{^{1}H} NMR spectrum. ^{31}P{^{1}H} (109.4 MHz): δ 14.8(s). MS (EI+): *m*/*z* 306 (M^+, base peak, correct isotopic pattern), 271 (M − Cl, correct isotopic pattern), 189 ($C_{10}H_7P_2$).

$NapP_2O_4H_2$ (5b). Water (0.5 cm^3) in DME (5 cm^3) was added to an externally cooled (0 °C) stirred suspension of $Nap(PCl_4)(PCl_2)$ **1b** (1.25 g, 3.12 mmol) in DME (20 cm^3) during 20 min. The reaction mixture was left to warm to ambient temperature, stirred for 1 h, and evaporated in vacuo to yield crude material, which was washed with thf (5 cm^3) and then extracted with more thf (30 cm^3); evaporation of extract in vacuo gave **5b** in the form of off-white solid, slightly contaminated with oxidized byproduct **5a**. Yield: 0.44 g (56%). NMR (CD_3OD, for numbering of atoms see Scheme 4): ^{1}H (300 MHz) δ 7.73−7.57 (m, 2H, H3 and H7), 8.05 [dd, integral intensity low as a result of H−D exchange, ^1J(HP^{III}) = 626, ^3J(HP^{III}) = 5.0 Hz, H11], 8.24−8.02 (m, 4H, H2, H4, H6 and H8); ^{13}C{^{1}H} (67.9 MHz) δ 122.6 [d, ^1J(CP) = 115.2 Hz], 123.1 [d, ^1J(CP) = 182.7 Hz], 126.0 [d, *J*(CP) = 15.6 Hz], 126.3 [d, *J*(CP) = 15.6 Hz], 130.1 [t, *J*(CP) = 11.4 Hz], 132.2 [d,

J(CP) = 8.3 Hz], 132.7 [t, J(CP) = 11.4 Hz], 133.8 (s), 134.3 [d, J(CP) = 11.4 Hz], 135.3 (s); $^{31}P\{^1H\}$ (109.4 MHz) δ 6.4 (d, P^V), 18.3 (d, P^{III}), ^2J(PP) = 27.4, quick exchange of H11 atom to D caused splitting of a majority of the P^{III} signal into a 1:1:1 triplet of doublets [$^1J(P^{III}D)$ = 95.5 Hz] as well as a slight isotopic lower frequency shift of the P^{III} signal to δ 18.0; ^{31}P (109.4 MHz) δ 6.4 (dd, P^V), 18.3 (ddd, P^{III}), ^2J(PP) = 27.4, $^3J(P^VH)$ = 17.0, $^1J(P^{III}H)$ = 626, $^3J(P^{III}H)$ = 18.4 Hz.

K[NapP$_2$O$_4$H] (6). The solution of the free acid **5b** (0.50 g) was titrated by aqueous solution of KOH to neutral pH, and the solid obtained after evaporation of water was extracted with hot ethanol (40 cm^3). The extract was concentrated to 5 cm^3, and the precipitated solid was recrystallized from a hot ethanol/methanol mixture. Yield: 90 mg (16%) of white hygroscopic microcrystalline **6**. Evaporation of mother liquor afforded another batch of **6**, which was however impurified by the dipotassium salt of **5a**. $C_{10}H_7P_2O_4K$: calcd C 41.1, H 2.4; found C 40.9, H 2.1. Mp: above 300 °C. IR (KBr tablet, cm^{-1}): ν = 3052w (ν_{Ar-H}), 2394m (ν_{P-H}), 1492s, 1271, 1253, 1243, 1232vs ($\nu_{P=O}$), 1120s, 1109s, 936s, 777s, 724s, 602s, 556s. Raman (sealed capillary, cm^{-1}): ν = 3054s (ν_{Ar-H}), 2397m (ν_{P-H}), 1572s, 1360vs, 1080m, 566s. NMR (D_2O, for numbering of atoms see Scheme 4): ^{1}H (300 MHz) δ 7.33 (m, 1H, H3), 7.44 (m, 1H, H7), 7.88 [dd, 1H, ^1J(P1−H) = 621, ^3J(H−P9) = 4.0 Hz, H1], 7.91−7.67 (m, 4H, H2, H4, H6 and H8); $^{13}C\{^1H\}$ (75.5 MHz) δ 121.5 [dd, ^1J(CP) = 123.2, ^3J(CP) = 5.9 Hz, C1], 125.8 [d, ^3J(CP) = 15.6 Hz, C3], 126.6 [d, ^3J(CP) = 15.8 Hz, C7], 126.1 [d, ^1J(CP) = 180.6 Hz, C9], 129.7 [t, J(CP) = 11.4 Hz, C10], 131.0 [d, ^2J(CP) = 8.3 Hz, C8], 132.3 [t, J(CP) = 11.8 Hz, C5], 132.9 (s, C6), 133.7 [d, ^2J(CP) = 12.2 Hz, C2], 135.5 (s, C4); $^{31}P\{^1H\}$ (109.4 MHz) δ 6.7(d, P^V), 22.2 (d, P^{III}), ^2J(PP) = 24.7, exchange of H11 atom to deuterium caused splitting of the P^{III} signal into a 1:1:1 triplet of doublets [^1J(PD) = 94.5 Hz] as well as a slight isotopic lower frequency shift of the P^{III} signal (δ_{PIII} 21.8 ppm); ^{31}P (109.4 MHz) δ 6.7 (dd, P^V), 22.2 (ddd, P^{III}), ^2J(PP) = 24.7, $^3J(P^VH)$ = 17.0, $^1J(P^{III}H)$ = 621, $^3J(P^{III}H)$ = 18.3 Hz. MS (ESI−): m/z 253 (anion, base peak), accurate mass measurement on $^{12}C_{10}{}^1H_7{}^{16}O_4{}^{31}P_2$ requires 252.9820, found 252.9824 (error of 1.7 ppm). MS (ES+): m/z 623 [(anion)$_2K_3^+$], 331 (anionK_2^+), 293 (anionHK^+), 255 (anionH_2^+), 237 (anion − O).

Polymer [(NapP$_2$O)$_2$O]$_n$ (7). To a stirred solution of Nap(PCl$_2$)$_2$ **1c** (2.73 g, 8.28 mmol) in thf (20 cm^3) was added water (0.6 cm^3, 33.3 mmol) in thf (6 cm^3) for 1 h at −80 °C. The reaction mixture was left to heat up slowly to ambient temperature and stirred for an additional 12 h. Precipitated solid was filtered off, washed with water (4 × 12 cm^3) and thf (2 × 10 cm^3), and dried in vacuo. Yield 0.82 g (70%) of the polymer **7** as pale yellow solid, insoluble in common organic solvents and in water. IR (KBr tablet, cm^{-1}): ν = 3055w, 3041w (ν_{Ar-H}), 2670wb ($\nu_{P(O)(OH)}$), 2266wb, 1607mb, 1488m, 1166s ($\nu_{P=O}$), 998s, 954vs (ν_{P-O-P}), 942vs, 818s, 771vs;

Cs$_2$[(NapP$_2$O$_2$)$_2$] (8). The suspension of polymer **7** (0.60 g, 1.41 mmol) in water was slowly titrated by ca. 10% solution of cesium hydroxide until only a small amount of solid remained undissolved (pH should not exceed 10). The cloudy solution was then filtered using filtration aid (Celite) and evaporated in vacuo to yield pale yellow solid. Its recrystallization from a small amount of methanol gave the cesium salt as a pale yellow, extremely oxygen-sensitive powder (0.53 g, 49%). The crystals of *rac*-**8**·2CH$_3$OH suitable for X-ray work were obtained by slow diffusion of diethyl ether into concentrated solution of **8** in methanol. $C_{20}H_{12}P_4O_4Cs_2$: calcd C 34.0, H 1.7; found C 33.7, H 2.0. Mp dec above 290 °C without melting. NMR (d_4-MeOH, major diastereomer, subtracted from its mixture with 7% of minor diastereomer, for numbering of atoms see Scheme 5): ^{1}H (300.1 MHz) δ 3.22 (s, variable amount, solvated methanol), 6.65 [m, 2H, ^3J(HH) = 8.3 and 7.0 Hz, H7], 7.06 [m, 2H, ^3J(HH) = 7.0, ^4J(HH) = 0.9 Hz, H8], 7.29 [m (≈d), 2H,^3J(HH) = 8.3, ^4J(HH) = 1.0 Hz, H6], 7.41 [m, 2H, ^{3}J(HH) = 8.1 and 6.8 Hz, H3], 7.59 [m (≈d), 2H,^3J(HH) = 8.3, ^4J(HH) = 1.0 Hz, H4], 7.70 [m (≈ddd), 2H, ^3J(HP) = 11.3, ^3J(HH) = 6.9, ^4J(HH) = 1.0 Hz, H2]; $^{13}C\{^1H\}$ (75.5 MHz) δ 50.3 (s, MeOH), 126.3 [m (≈t), ^2J(CP) + ^3J(CP) = 5.0 Hz, C2], 126.9 (m, C7), 127.7 [t, ^3J(CP) + ^4J(CP) = 11.6 Hz, C3], 128.6 (s, C6), 130.8 [t, ^4J(CP1) + ^4J(CP9) = 2.8 Hz, C4], 133.1−133.9 [2 × m (overlapped), C5 and C8], 134.6 (m, C9), 138.3 (m, C10), 142.8 (m, C1); $^{31}P\{^1H\}$ (121.5 MHz) AA′XX′ system, simulation yielded δ_A −77.9 and δ_X 52.8, $^1J(P^IP^I)$ = −245.5, $^1J(P^IP^{IV})$ = −136, $^2J(P^IP^{IV})$ = 22.0, $^3J(P^{IV}P^{IV})$ = −25.5 Hz; signals of second diastereomer (ca. 7% of integral intensity) with δ_A −79.7 and δ_X 55.6 were observed as additional AA′XX′ system. IR (Nujol mull, cm^{-1}): ν = 3052w and 3037w (ν_{Ar-H}), 1487m, 1189, 1181, 1172, 1162vs ($\nu_{P=O}$), 1054, 1036, 1025vs, 816m, 773s, 597s, 540s, 489s, 444m. Raman (sealed capillary, cm^{-1}): ν = 3053m (ν_{Ar-H}), 1564vs, 1382vs, 1063s, 883s, 544s, 531m, 435m, 288m. MS (ES−, sampled as the solution in MeOH): m/z 589 (anion + Cs + O), 573 (anion + Cs), 441 (anion + H)$^-$, 283 ($NapP_2O_5Me$ − hydrolysis/oxidation product, base peak), 220 (anion^{2-}).

Acknowledgment. The authors thank EPSRC for an equipment grant.

Supporting Information Available: Tables (in CIF format) giving atomic coordinates, anisotropic thermal parameters, bond lengths, and bond angles for compounds **3a**, **3b**, and *rac*-**8**. This material is available free of charge via the Internet at http://pubs.acs.org.

IC035364H